Study of intense rainfall events over India using Kalpana-IR and TRMM-precipitation radar observations

Anoop Mishra*, R. M. Gairola, A. K. Varma and V. K. Agarwal

Oceanic Sciences Division, Meteorology and Oceanography Group, Space Applications Centre, ISRO, Ahmedabad 380 015, India

An attempt has been made here to analyse the infrared (IR) radiances from Kalpana/INSAT data along with the high resolution rainfall estimates from Precipitation Radar onboard Tropical Rainfall Measuring Mission (TRMM) satellite. Contrary to the IR, microwave rain (MW) rates are based on measurements that sense precipitation in clouds and do not rely on cloud top temperature. The combination of the broad coverage and frequent refresh of the geostationary satellites with the sparse but more accurate active MW rain rates has been used for the characterization of precipitation-bearing systems over Indian land from adjoining oceans. These studies are taken up to enhance the capability of rainfall retrievals in the near future using synergy from both INSAT-3D and Megha-Tropiques, IR and MW measurements respectively. The intercomparison with TRMM-3B42 and the validations with the rain-gauges and Doppler Weather Radar shows that the present technique is able to retrieve the rainfall with reasonable good accuracy.

Keywords: Hydrology, infrared, passive microwave, precipitation, remote sensing.

ACCURATE estimation of rainfall at small spatial (few km) and temporal scales (hourly, three-hourly or subdaily) has many applications in meteorology and hydrology. Using a combination of ground-based radars and dense network of rain gauges, such information is available but only over limited areas. Continuous high temporal resolution satellite data uniformly over a large area is available only from instruments onboard geostationary platforms. This restriction currently limits available spectrum of electromagnetic wavelength to those in the infrared (IR) and visible (VIS) part of electromagnetic spectrum. The lack of visible data at night has generally restricted geostationary rainfall monitoring technique to the use of IR data alone. Though the satellite IR algorithms benefit from high temporal sampling, the IR radiances eminating from cloud tops have only an indirect relationship with surface rainfall which, in turn, results in weak statistical relationships between rainfall and cloudiness. The most common technique for the IR rain estimate counts cloudy pixels within a given area that are colder than a given threshold temperature (e.g. 235 K in cloud indexing method by Arkin *et al.*[1]). The pixels that are colder than threshold temperature are probably associated with precipitating convective clouds possessing cold high tops. But there are some sources of errors, e.g. high-level cirrus and other non-precipitating clouds often screened in as precipitating with this simple relationship. Further, Arkin *et al.*[2] estimated precipitation over Indian region from IR window channel observation of INSAT-1B using simple cloud indexing technique. Bhatt and Nakamura[3] showed the complex diurnal variability in convection and rainfall around the highest mountains (Himalayan) all over the world. Recently, Sarkar *et al.*[4] applied ANN approach to improve the quality of INSAT derived Quantitative precipitation estimation (QPE) over the Indian region for the summer monsoon. Stephans *et al.*[5] presented a critical review of a number of popular methods that have been developed to retrieve cloud and precipitation properties from satellite radiance measurements.

Precipitation Radar (PR) onboard TRMM is the first spaceborne radar that gives the three-dimensional structure of rainfall. PR is able to provide significantly more accurate estimation of rainrates but suffers from poor temporal sampling associated with platforms in low earth orbits. Due to the low sampling rate, such instruments are most suitable for the estimation of accumulated rainfall over longer periods.

Houze *et al.*[6] analysed the monsoon convection over the Himalayan region using TRMM PR data. However, these measurements could be highly valuable in using its instantaneous rain estimates to calibrate the IR-brightness temperature (TBs) for rainfall estimation. For this purpose, many attempts are being made worldwide recently to integrate IR and microwave (MW) observations. Some such algorithms were described by Gairola and Krishnamurti[7], Mitra *et al.*[8] and Todd *et al.*[9]. An adjusted global precipitation index (AGPI) technique was developed by Adler *et al.*[10], in which a correction factor is derived from the comparison of Passive Microwave (PMW) and Global Precipitation Index (GPI) estimates for coincident time slots over some extended periods (e.g. one month). This correction is then applied to all the hourly GPI estimates during that period. Xu *et al.*[11] extended this technique to develop the Universally Adjusted GPI (UAGPI) method in which both the monthly IR thresholds and IR conditional rain rate are optimized using coincident PMW and IR data.

An optimal combination of highly accurate MW observations from PR with TB from geostationary IR observations that are available in nearly the same spatial scale can be exploited to obtain the maximum accurate rainfall information. This has been the thrust area for many meteorological applications as a primary scope of the present work.

In the present study, we use the PR estimated rainfall along with Kalpana-IR TB over the same region and the

*For correspondence. (e-mail: anoopmishra_1@yahoo.co.in)

same period in the same grid boxes of $0.25° \times 0.25°$ for creating a matched database for the regression analysis over the Indian land and oceanic regions. The regression equation is then applied for the estimation of 3-hourly to daily rainfall using the Kalpana-IR brightness temperature data. Comparisons with operational rainfall product from TRMM (3B42) have been carried out as independent verification of the present approach. Further, the validations with the rain-gauges and Doppler Weather Radar (DWR) have been attempted.

Kalpana satellite is a dedicated, meteorological geostationary satellite launched by Geo-Stationary Launch Vehicle (GSLV) and operating since 24 September 2002. This geostationary satellite carries onboard a Very High Resolution Radiometer (VHRR) along with other instruments. This sensor operates in three wavelengths bands, viz. VIS, TIR and WV. In WV and TIR bands, the spatial resolution is 8 km whereas in VIS band spatial resolution is 2 km. The VHRR frequency bands are given as: (i) thermal IR band-TIR: 10.5–12.5 μm, (ii) visible band-VIS: 0.55–0.75 μm and (iii) water vapour band-WV: 5.7–7.1 μm.

The details of the Kalpana satellite are given by Kaila *et al.*[12]. In the present study, we used the Kalpana-IR data during July 2006 and June 2007.

The TRMM is a joint US–Japan Satellite Mission to monitor tropical and subtropical precipitation and to estimate its associated latent heating. It was launched in late November 1997 into a near circular orbit approximately at 350 km altitude (raised to 420 km since 2001) at 35° inclination from the equatorial plane. The description and details of the TRMM sensors and products are described by Kummerow *et al.*[13]. We use the data from PR(2A25) (ref. 14), onboard TRMM and a merged IR and MW data product called 3B42 (ref. 15) for the present study. PR, the first of its kind in space, is a 2 m active phased array radar system operating at 13.8 GHz. The PR scans across a 215 km swath width with 80 vertical range bins extending to 20 km above the earth ellipsoid. The vertical and horizontal resolutions are 250 m and 5 km respectively at nadir. The data during July 2006 and June 2007 were used for the present study.

Another operational TRMM data set used in the present study is called 3B42, which is a merged product from Geostationary IR and MW data. The data from TRMM satellite are archived and distributed by the NASA Goddard DAAC. The data of July 2006 and June 2007 were downloaded from the site for the intercomparison of the present technique.

The Indian Space Research Organization (ISRO) designed AWS as a very compact, modular, rugged, powerful and low-cost system and housed in a portable, self-contained package. Among many other sensors, it has a tipping bucket rain gauge with a magnet and reed switch with unlimited rain measuring capacity with accuracy of less than 1 mm. AWS transmits its hourly meteorological data in burst of 68 ms duration (at a data rate of 4.8 kbps). At present, there are about 300 AWS operationally working all over India. INSAT Data Collection Platform is used for data acquisition. More details are given in Vashistha *et al.*[16].

For the validation of the present algorithm, AWS rain gauge data obtained during 2007 is used. The point measurements by AWS are averaged within $1° \times 1°$ grids similar to present observations. AWS map is shown in Figure 1.

DWR is an indigenously developed S-band radar over India at Sriharikota at 13°60′N and 80°23′E location. It is capable of monitoring clouds, precipitation systems and winds over large areas of more than 400 km from the radar location. DWR has the unique capability to continuously track and predict fast evolving weather systems such as thunderstorms, cyclones and cloudbursts. The RADAR reflectivity factor z from the DWR is taken as the base product for the present study. The DWR rain values have been derived using Z–R relationship developed during the campaign using disdrometer data at the site. Rainfall measured using DWR depends upon the empirical exponential relationships between the radar reflectivity factor z and the rainrate R through the relationship $z = aR^b$, where constants a and b vary over different regions and the rain regimes. The DWR values are available in the scan radius of 614 km with the scan resolution of 300 m with the display range of 614 km. Display grid size is 2×2 km and the pulse width is 2 μs. A single scan of DWR covers 360° azimuth directions at one elevation. In the present study, 0.5° elevation data of DWR during the post-monsoon months of the years 2007 and 2008 were used to produce the surface rainfall for the comparisons with the present technique.

Observations from PR at 5 km resolution offer a unique opportunity to enhance the capability of the retrieval of rainfall from IR sensors of almost similar resolution. The three-dimensional structure of rainfall from PR also provides an opportunity for surface effects (emission/reflection) to be eliminated by considering the height above-the-ground (say 1.5 to 2 km). In the present study, the precipitation rates from TIR-TBs are derived using a power-law fit between instantaneous PR derived rainfall estimates and satellite measurements of the IR-TBs at cloud top. This is carried out by collocating Kalpana-IR TBs from the cloud tops with PR derived rain rates in $0.25° \times 0.25°$ grid over the Indian region between 20°S–40°N and 50–120°E during July 2006 and June 2007. After analysing many convective systems over several days during these times, 1364 collocated and concurrent grids consisting of IR cloud-tops temperature and corresponding instantaneous PR rainfall rate estimates were collocated from 14 pairs of observations (during pre-monsoon, monsoon and post-monsoon). This data set was used to compute the regression between the mean precipitation radar derived rainfall rate and IR-TB is given in the

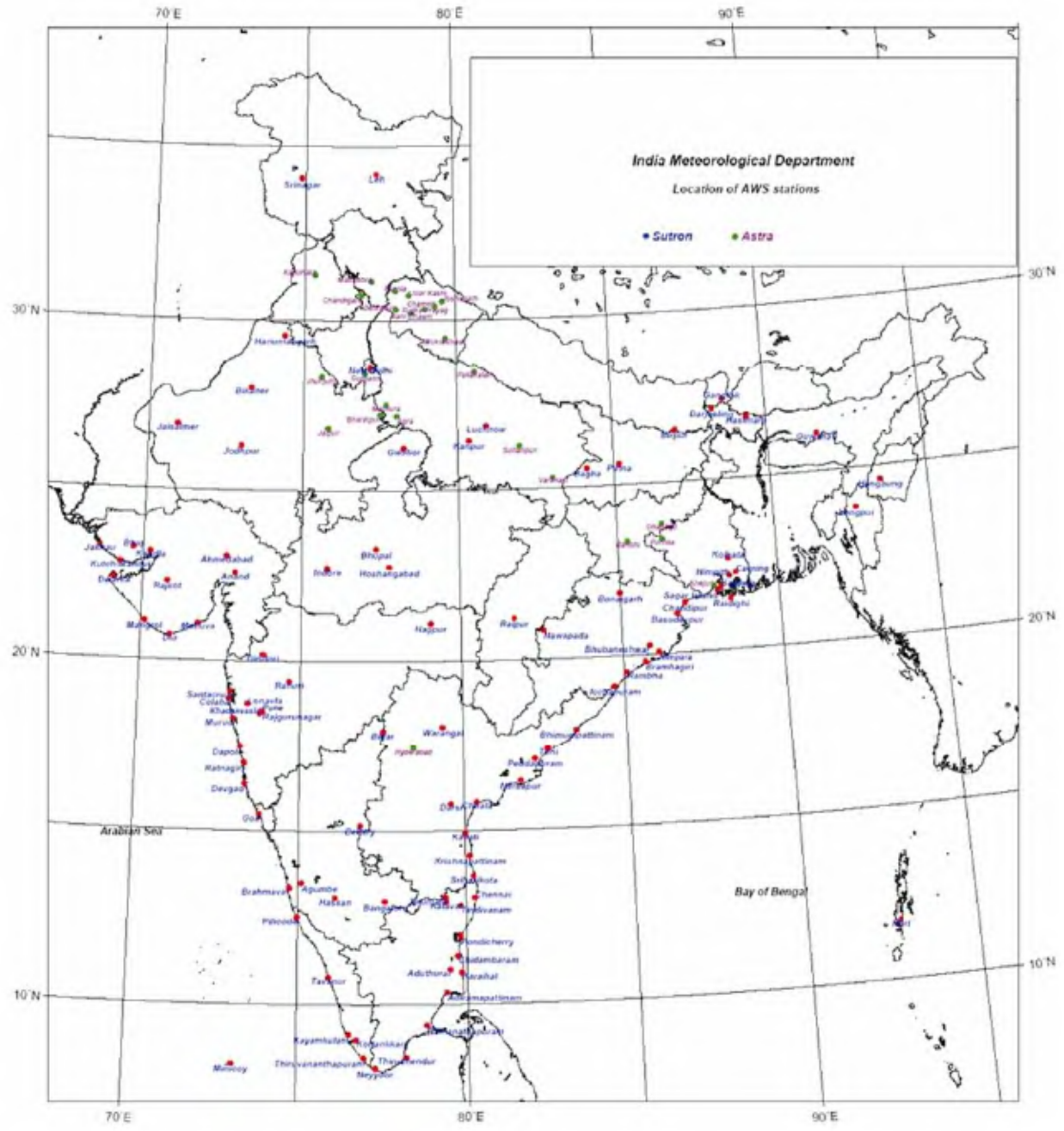

Figure 1. AWS rain gauge distribution over India.

Figure 2. The curve representing the regression fit is given as:

$$R = 4.47804 \times \exp(-(\mathrm{TB} - 194.219)/28.5426),$$

where R is the rain rate in mm/h and TB the cloud top brightness in Kelvin.

The standard error of estimates of the curve is 4.24 and the correlation coefficient is 0.715.

As stated earlier, the set of IR and MW measurements from Kalpana and TRMM satellites have been used for the rainfall estimation algorithm. The algorithm was tested for the Indian land and oceanic regions during July 2006 and June 2007, and the performance of the algorithm was validated with rain-gauges and TRMM-3B42 data. The validation results show that the present technique is far more superior than the one being used by the India Meteorological Department (IMD) for operational purposes based on the Arkin's method. Some of the results are discussed below.

There were two intense convective systems along Indo-Gangetic plane on 8 July 2006. Figure 3 *a* shows TB's

Table 1. Comparison statistics between the GPI and the present technique with the rain gauge

	No. of grid points	Correlation coefficient (%)	Bias (mm)	Root mean square error (mm)
GPI technique	97	0.30	–3.98	23.23
Present technique	97	0.60	–2.53	22.34

Table 2. Comparison statistics between the GPI and the present technique with the TRMM-3B42

	No. of grid points	Correlation coefficient (%)	Bias (mm)	Root mean square error (mm)
GPI technique (daily rainfall, eight images per day)	687	0.55	–2.94	11.82
Present technique (3-hourly rainfall)	61,920	0.76	–0.235	1.73

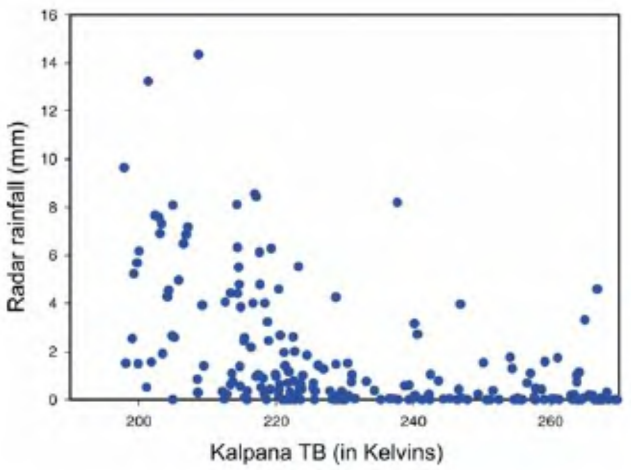

Figure 2. Scatter plot between Kalpana brightness temperature and RADAR rainfall.

Table 3. Comparison of rainfall from DWR and rainfall from the present technique

No. of data points	895
Correlation coefficients	0.75
Root mean square error (mm)	2.37
Bias (mm)	0.6514

plot on that day. These convective systems are associated with the heavy rainfall as reported by IMD. Figure 3 *b* shows the three-hourly rainfall estimates from the present technique. A rain amount of 30–50 mm/3 h is obtained in the central UP region and that matches quite closely in its position and amount obtained from TRMM 3B42 (Figure 3 *c*). It is observed that although low rainfall values (less than 9 mm/3 h) are well picked up by the Arkin's technique, high rainfall values are underestimated by this technique (Figure 3 *d*). This is the biggest limitation of the Arkin's technique.

Even though one of the convective systems at 28°N and 80°E was highly localized, the present technique is able to retrieve the rainfall properly.

The second case study, which was carried out for 9 July 2006 at 0600 UTC, was aimed to examine the performance of our algorithm for spatially variable rain rates over the area of study. Figure 4 *a* shows the TB's plot, which indicates that there were three systems: one at northern part of India (30°N, 78°E), other at the Head Bay of Bengal (20°N, 90°E), and third one at the northern part of Vietnam (22°N, 108°E). Figure 4 *b* represents the rainfall plot obtained using the present technique. From the figure, one can see that rainfall associated with these systems are 20–30 mm/3 h, 10–20 mm/3 h, and 10–20 mm/3 h for systems located at 30°N and 78°E, 20°N and 90°E and 22°N and 108°E respectively. The location and rain amounts are in good agreement from the rainfall obtained from the TRMM-3B42 (Figure 4 *c*) except at 22°N and 108°E, where rainfall from TRMM-3B42 is in the range of 40–60 mm/3 h, but from the present technique this amount is in the range of 20–40 mm/3 h.

Apart from these convective systems, some other systems (e.g. at 4°N, 68°E and 4°N, 94°E) associated with small amount of rainfall (i.e. 10 mm/3 h) were also well picked up by the present technique and they are in agreement with the rainfall amounts observed from TRMM-3B42. Again it was observed from the Arkin's method (Figure 4 *d*) that higher rainfall values (greater than 9 mm/3 h) were underestimated.

Further, we have validated our results with AWS rainfall averaged in the same grid and TRMM-3B42 data. For the comparison with operational GPI technique used by IMD, we have also applied this technique to Kalpana data and compared the results with AWS and TRMM-3B42 rain values. These comparisons are shown in Figure 5 and the relevant statistics are given in Tables 1 and 2. The results show that the present approach is able to retrieve the rainfall with more accuracy than the GPI technique.

Figure 6 shows the statistical comparison between the rainfall from DWR observation and that from the present technique. A total of 895 data points during the selected cases of 2007 and 2008 were considered after averaging them in $0.25° \times 0.25°$ grid boxes. Table 3 shows the sta-

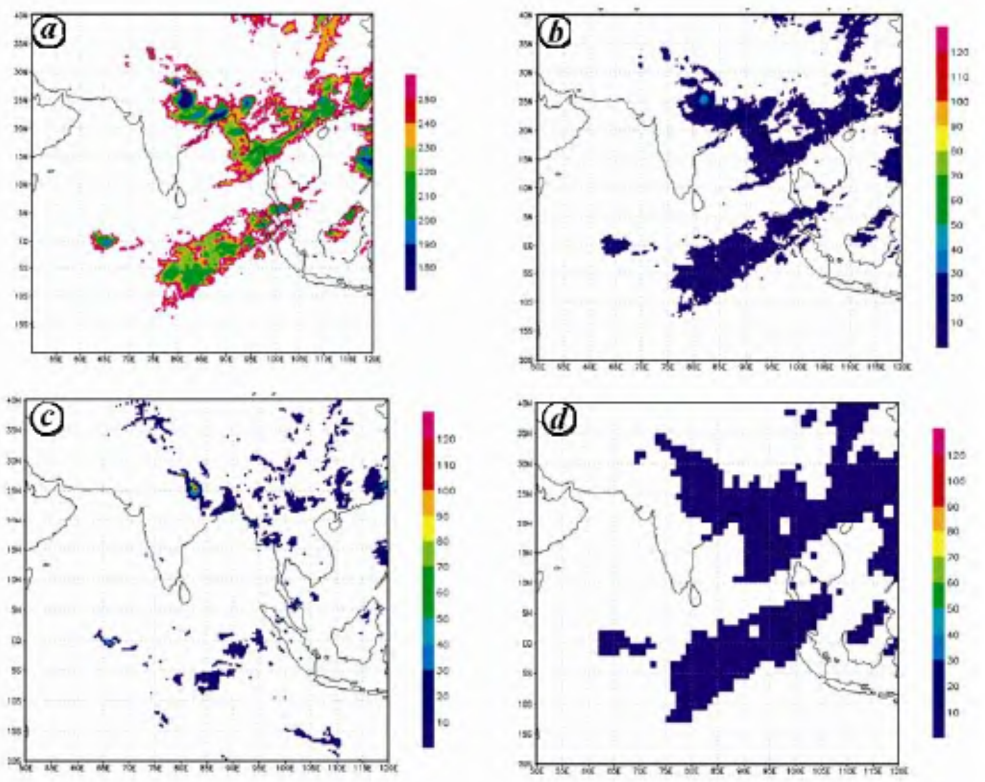

Figure 3. ***a***, Brightness temperature, 8 July 2006 at 1200 UTC. ***b***, Rainfall from the present technique, 8 July 2006 at 1200 UTC. ***c***, Rainfall from TRMM-3B42, 8 July 2006 at 1200 UTC. ***d***, Rainfall from Arkin's method, 8 July 2006 at 1200 UTC.

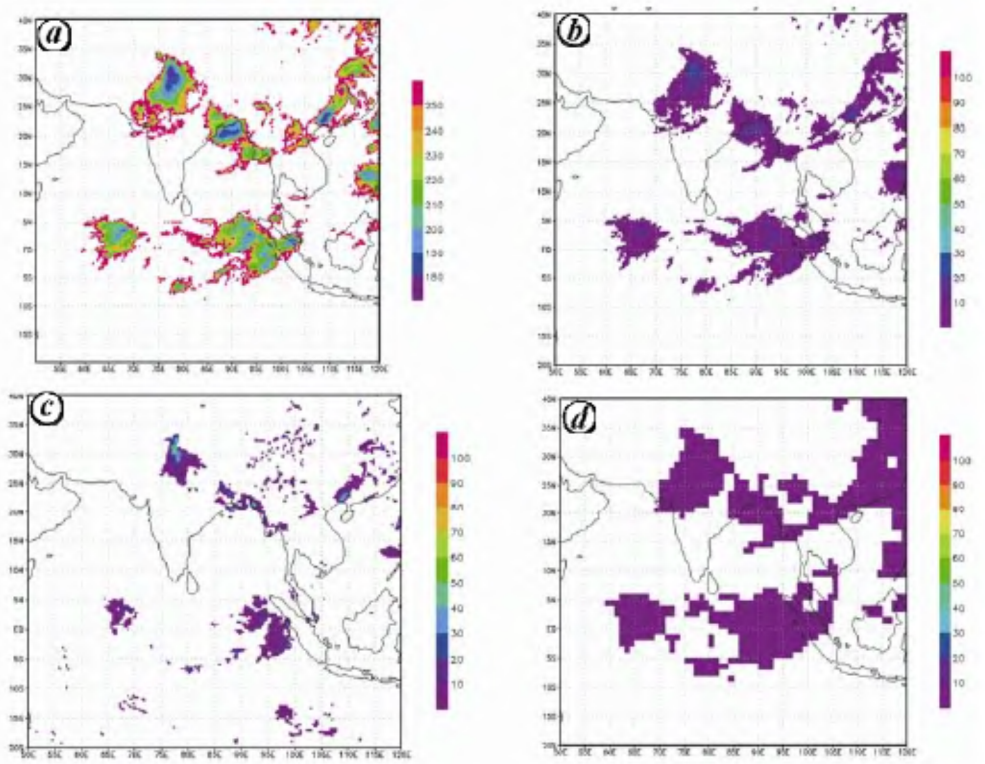

Figure 4. ***a***, Brightness temperature, 9 July 2006 at 0600 UTC. ***b***, Rainfall from the present technique, 9 July 2006 at 0600 UTC. ***c***, Rainfall from TRMM-3B42, 9 July 2006 at 0600 UTC. ***d***, Rainfall from Arkin's method, 9 July 2006 at 0600 UTC.

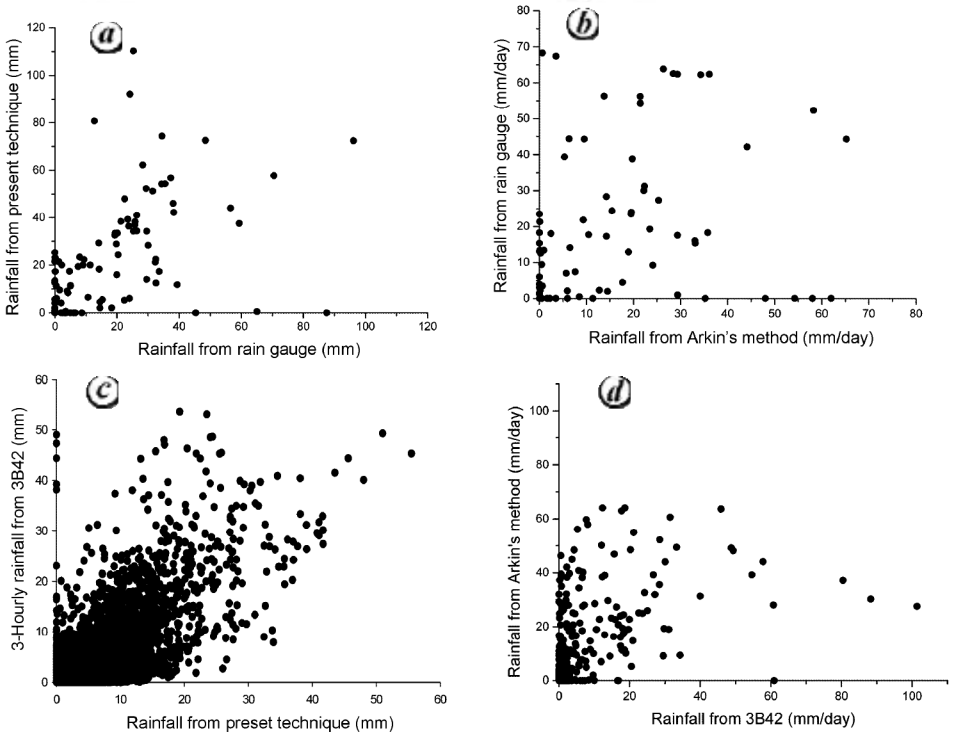

Figure 5. Scatterplots of gauge vs the present technique (*a*); gauge vs GPI technique (*b*); TRMM-3B42 vs the present technique (*c*), and TRMM-3B42 vs GPI technique (*d*).

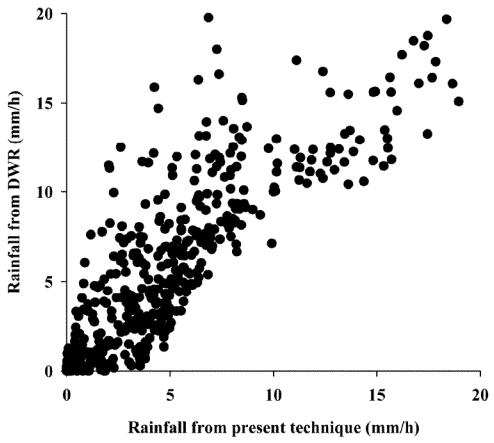

Figure 6. Scatter plot between the rainfall from DWR observation and the rainfall from the present technique.

tistical comparison of these two observations. The correlation coefficients between the rainfall from RADAR observation and the rainfall from the present technique is 0.75, root mean square error is 2.37 mm/h while the bias is 0.6514 mm/h. So it is clear from the above results that the present technique is able to retrieve the rainfall with good accuracy.

This communication describes the development of a rainfall estimation technique based on both IR and MW observation from Kalpana and TRMM-PR data. The rain rate is derived using a power-law regression relationship between the Kalpana-IR-TB's and the PR-rain-rate. Validation has been performed using the merged IR and MW (TRMM-3B42) observations, AWS rain-gauge and DWR observations. The present technique has proved that availability of satellite MW PR data (from low orbiting satellites) can improve the performance of IR-based rainfall significantly in the areas where there is lack of sufficient ground rainfall observations. The validation results show that the present technique is able to retrieve the rainfall with more accuracy than the GPI technique. This study is taken up to enhance the capability of rainfall estimation in the near future using synergy from both INSAT-3D and Megha-Tropiques, IR and MW measurements respectively. In future, we also plan to develop the standardized rain estimation technique based on data with longer periods for different regions of India. Further, TRMM-3B42 being an estimate itself, might have certain problems over India during monsoon seasons, so we plan more work on evaluating this product over India in future.

1. Arkin, P. A. *et al.*, The relationship between fractional coverage of high cloud and rainfall accumulations during GATE over the B-scale array. *Mon. Weather Rev.*, 1979, **107**, 1382–1387.
2. Arkin, P. A., Krishna Rao, A. V. R. and Kelkar, R. R., Large scale precipitation and outgoing longwave radiation from INSAT-1B during the 1986 South West Monsoon season. *J. Climate*, 1989, **2**, 619–128.

3. Bhatt, B. C. and Nakamura, K., Characteristics of monsoon rainfall around the Himalayas revealed by TRMM precipitation radar. *Mon. Weather Rev.*, 2005, **133**, 149–165.
4. Nath, S., Mitra, A. K. and Bhowmik, R. S. K, Improving the quality of INSAT derived quantitative precipitation estimation using a neural network method. *Geofizika*, 2008, **25**, 43–51.
5. Stephans, G. L. and Kummerow, C. D., Remote sensing of clouds and precipitation from space: a review. *J. Atmos. Sci.*, 2006, **1**, 3742–3765.
6. Robert, A., Houze Jr, R. A., Wilson, D. C. and Small, F., Monsoon convection in the Himalayan region as seen by the TRMM Precipitation Radar. *Q. J. R. Meterol. Soc.*, 2007, **133**, 1389–1411.
7. Gairola, R. M. and Krishnamurthy, T. N., Rain rates based on SSM/I, OLR and rain gauge data sets. *Meteorol. Atmos. Phys. (Austria)*, 1992, **50**, 165.
8. Mitra, A. K., Das Gupta, M., Singh, S. V. and Krishnamurti, T. N., Daily rainfall for Indian monsoon region from merged satellite and rain gauge values: large scale analysis from real time data. *J. Hydrometeorol.*, 2003, **4**, 769–781.
9. Todd, M. C., Barrett, E. C., Beaumont, M. J. and Green, J., Satellite identification of rain days over the upper Nile river basin using an optimum infrared rain/no rain threshold temperature model. *J. Appl. Meteorol.*, 1995, **34**, 2600–2611.
10. Adler, R. F., Huffman, G. J. and Keehn, P. R., Global rain estimates from microwave adjusted geosynchronous IR data. *Remote Sensing Rev.*, 1994, **11**, 125–135.
11. Xu, L., Gao, X., Sorooshian, S., Arkin, P. A. and Imam, B., A microwave infrared threshold technique to improve GOES precipitation index. *J. Appl. Meteorol.*, 1999, **38**, 569–579.
12. Kaila, V. K., Kiran Kumar, A. S., Sundarmurthy, T. K., Ramkrishnan, S., Prasad, M. V. S., Desai, P. S., Jayaraman, V. and Manikiam, B., METSAT – a unique mission for weather and climate. *Curr. Sci.*, 2002, **83**, 1081–1088.
13. Kummerow, C., The status of the tropical rainfall measuring mission (TRMM) after two years in orbit. *J. Appl. Meteorol.*, 2000, **39**, 1965–1982.
14. Iguchi, T., Kozu, T., Meneghini, R., Awaka, J. and Okamoto, K., Preliminary results of rain profiling with the TRMM precipitation radar. Proceedings of the Eighth Open Symposium on Wave Propagation and Remote Sensing, International Union of Radio Science Commission F, Aveiro, Portugal, 1998, pp. 147–150.
15. Huffman, G. J. *et al.*, The TRMM multisatellite precipiatation analysis (TMPA): quasi-global multiyear, combined-sensor precipitation estimates at fine scales. *J. Hydro. Meterol.*, 2007, **8**, 38–55.
16. Vashistha, R. D. and Srivastava, S. K., Automatic weather station for collecting meteorological data for urban areas, WMO technical conference on instruments and methods of observations (TECO-2000), 2000.
17. Kummerow, C., Barnes, W., Kozu, T. and Simpson, J., The Tropical Rainfall Measuring Mission (TRMM) sensor package. *J. Atmos. Oceanic Technol.*, 1998, **15**, 809–817.

ACKNOWLEDGEMENTS. We thank Director, Space Applications Centre for the encouragement. The TRMM data from NASA/GSFC used in the study is acknowledged.

Received 10 October 2008; revised accepted 7 July 2009

Genetic diversity assessment in intra- and inter-populations of *Xylocarpus granatum* Koen.: a critically endangered and narrowly distributed species of Maharashtra

Smita B. Jugale[1], Leela J. Bhosale[1,*], Trupti D. Kad[2] and A. B. Nadaf[2]

[1]Department of Botany, Shivaji University, Kolhapur 416 004, India
[2]Department of Botany, University of Pune, Pune 411 007, India

The threatened mangrove species *Xylocarpus granatum* Koen. has been rediscovered after a period of nine decades from the West Coast of Maharashtra. On the basis of IUCN guidelines, the species is categorized as a critically endangered and narrowly distributed species of Maharashtra. When the inter- and intra-populations spread across the estuaries of Maharashtra Coast were studied, it was observed that the species shows considerable phenotypic variation with respect to leaflet size and shape, number of floral parts, number and size of fruits per inflorescence, and also dimorphism in leaves. Hence, populations of *X. granatum* from three different localities representing the above-mentioned phenotypic variations were selected and assessed at biochemical level by protein profiling and at genomic level using ISSR markers. The analyses showed that even though the variation exists at phenotypic level, the inter- and intra-populations showed similarity in total protein pattern and 92% similarity at genomic level. Thus, it seems that the phenotypic variations in the inter- and intra-populations of *X. granatum* are probably epigenetic. The low genetic variation in this species threatens its own existence and strongly demands immediate appropriate conservation measures.

Keywords: ISSR markers, intra- and inter-population variations, morphological variation, *Xylocarpus granatum* Koen.

THE mangrove genus *Xylocarpus*, belonging to the family Meliaceae, has three distinct species: *X. granatum* Koen., *X. moluccensis* Lamk. and *X. mekongenesis* Pierre., that are distributed in tropical tidal forests of Old World, typical mangrove habitat or in sandy or coastal habitats spread from Africa to Australia, including India and Malayan Archipelago[1]. In India, these three species were recorded from Andaman Islands[2] and Orissa Coast[3] whereas the two species, *X. granatum* Koen. and *X. mekongenesis* Pierre. were reported from Sundarbans[4], Tamil Nadu Coast[5] and Andhra Pradesh[6], and one species *X. granatum* Koen. from Maharashtra[7–9]. In Maharashtra, *X. granatum* Koen. has been reported by Cooke[10] and

*For correspondence. (e-mail: ljbhosale@yahoo.com)